International Journal of Pharmaceutics 427 (2012) 177–184

Contents lists available at SciVerse ScienceDirect

International Journal of Pharmaceutics

journal homepage: www.elsevier.com/locate/ijpharm

Controlled synergistic delivery of paclitaxel and heat from poly(β-amino ester)/iron oxide-based hydrogel nanocomposites

Samantha A. Meenach[a,1], Chinedu G. Otu[b], Kimberly W. Anderson[a], J. Zach Hilt[a,*]

[a] Department of Chemical & Materials Engineering, University of Kentucky, 177 F. Paul Anderson Tower, Lexington, KY 40506, USA
[b] Department of Biology, University of Kentucky, 101 Morgan Building, Lexington, KY 40506, USA

ARTICLE INFO

Article history:
Received 6 January 2011
Received in revised form 20 January 2012
Accepted 24 January 2012
Available online 1 February 2012

Keywords:
Hydrogel
Nanocomposites
Poly(β-amino ester) (PBAE)
Hyperthermia
Paclitaxel
Cancer

ABSTRACT

Poly(β-amino ester) (PBAE) biodegradable hydrogels were investigated for potential combined chemotherapeutic and heat delivery in the synergistic treatment of cancer. Hyperthermia, the heating of cancerous tissue from 41 to 45 °C, increases the efficacy of conventional cancer therapies such as irradiation and chemotherapy. The hydrogel nanocomposites in this work provide a drug delivery vehicle (via the biodegradable PBAE polymer network) and the ability to be heated remotely upon exposure to an alternating magnetic field (via iron oxide nanoparticles incorporated into the hydrogel matrix). PBAE macromers composed of poly(ethylene glycol) (N = 400) diacrylate (PEG400DA) or diethylene glycol diacrylate (DEGDA) with isobutylamine (IBA) were synthesized. Hydrogel nanocomposites were fabricated via free-radical polymerization to form a bulk hydrogel matrix entrapping both iron oxide nanoparticles and paclitaxel. The 2EG–IBA hydrogel exhibited complete degradation after approximately 7 weeks whereas the 9EG–IBA hydrogel degraded completely in 11 h. The hydrogels heated upon exposure to an alternating magnetic field throughout the degradation process. Additionally, the cytotoxicity of the degradation products was evaluated. Paclitaxel release was controlled via bulk degradation of the hydrogels. The tailorability of these nanocomposites makes them solid candidates for the synergistic treatment of cancer.

1. Introduction

Cancer is currently the second leading cause of death in the United States. In 2009 alone, there were an estimated 1.5 million new cases diagnosed (ACS, 2009). Despite the amount of research being done to overcome this disease, there are still many types of cancer, such as glioblastoma and pancreatic cancer (Sneed et al., 1998), which have extremely poor treatment success rates. Therefore, multiple-modality treatment has become the preferred treatment approach in the clinical setting. Most patients receive multiple types of treatment, including surgery, chemotherapy, or radiation. Hyperthermia, the heating of cancer tissues to between 41 and 45 °C, has been proven to provide a more effective way of treating some types of cancer in combination with well-developed therapeutics such as radiation and chemotherapy (Falk and Issels, 2001). Aside from having a cytotoxic effect on cancerous tissue, hyperthermia has been shown to increase tumor blood flow. This phenomenon can decrease hypoxia, acidosis, and energy deprivation at the tumor site which can thereby increase therapy efficacy as these conditions often make the treatment of cancer more difficult (Hildebrandt et al., 2002). Hyperthermia therapy faces a number of obstacles including the inability to restrict local heating of the tumor without damaging surrounding tissue (Moroz et al., 2002) or without using invasive and uncomfortable heating probes (Guedes et al., 2005). This can potentially be overcome through the development of systems which can be delivered to tumors and remotely heated from outside the body. We present a hydrogel nanocomposite capable of delivering both heat and a chemotherapeutic for local synergistic treatment of cancer through the implantation or in situ injection of the hydrogel within or near malignant tumors.

Hydrogel nanocomposites involve the incorporation of nanoparticulates within a hydrogel matrix which can enhance the properties of conventional hydrogel systems. A number of nanoparticulates have been utilized in nanocomposite hydrogel systems including metallic nanoparticles, carbon nanotubes, clay, ceramics, magnetic nanoparticles, hydroxyapatite, and semiconducting nanoparticles (Meenach et al., 2009b). Hydrogels are advantageous for many biomedical applications due to their resemblance of natural living tissue and inherent biocompatibility, which can be partially attributed to their soft, flexible nature

* Corresponding author. Tel.: +1 859 257 9844; fax: +1 859 323 1929.
E-mail addresses: s.meenach@uky.edu (S.A. Meenach), chinedu.otu@uky.edu (C.G. Otu), kanderson@engr.uky.edu (K.W. Anderson), hilt@engr.uky.edu (J.Z. Hilt).
[1] Present address: College of Pharmacy, Department of Pharmaceutics-Drug Development Division, University of Kentucky, 789 S. Limestone St., Lexington, KY 40536-0596, USA.

0378-5173/$ – see front matter © 2012 Elsevier B.V. All rights reserved.
doi:10.1016/j.ijpharm.2012.01.052

and high water content (Peppas et al., 2006). Magnetic hydrogel nanocomposites containing nanoscale superparamagnetic iron oxide nanoparticles have the potential to be used in hyperthermia therapy due to their ability to heat upon exposure to an alternating magnetic field (AMF). The heating mechanisms for these paramagnetic particles are based primarily on Brownian relaxation (rotation of the particle as a whole according to an external magnetic field), the Néel effect (reorientation of the magnetization vector inside the magnetic core against an energy barrier), and often some minimal hysteresis losses (Babincova et al., 2001). One of the advantages of using AMF for biomedical applications is that the field can pass through human tissue. Hydrogel nanocomposites containing iron oxide nanoparticles have already been utilized in applications such as remote-controlled drug delivery (Satarkar and Hilt, 2008), microfluidic valves (Satarkar et al., 2009), hydrogel degradation (Hawkins et al., 2009) and thermoablation (Meenach et al., 2009a,c).

In addition to delivering heat, these materials also have the potential to deliver therapeutic agents for cancer and other diseases. There are many disadvantages to using systemic chemotherapy delivery for cancer treatment including systemic toxicity, low drug bioavailability, and difficulty in delivering the drug(s) effectively into tumors (Ta et al., 2008). Hydrogel nanocomposites have the ability to overcome these obstacles through the local delivery of chemotherapeutic agents at therapeutic doses to increase treatment efficacy, likely in conjunction with systemic chemotherapy. In recent years, poly(β-amino ester) (PBAE) hydrogels have been investigated for biomedical applications such as drug delivery and tissue engineering. Anderson et al. have developed a combinatorial library of biodegradable crosslinkable polymers which characterizes various PBAE macromers. This library consists of acrylate-terminated poly(β-amino ester) macromers synthesized via a Michael addition reaction that combines primary or secondary amines with diacrylates (Anderson et al., 2006). There are many benefits to using such biodegradable hydrogel systems including: (1) monomer reagents that are inexpensive and commercially available, (2) macromer polymerization that can be completed without additional protection/deprotection schemes, and (3) no byproducts generated during the synthesis so that no purification steps are necessary (Anderson et al., 2006). Utilizing PBAE macromers in a hydrogel matrix can allow for hydrogel systems whose degradation, mechanical strength, and toxicity can be controlled based on the monomer reagents used.

Paclitaxel (PTX) is a plant alkaloid which effectively disrupts mitosis during the G2 phase of the cell cycle by binding with the β-subunit of tubulin dimers. This interferes with the dynamic instability of the microtubules in the cytoskeleton causing the cells form highly stable, rigid microtubules which prevents proliferation (Michalakis et al., 2007; Obara et al., 2005). PTX has been commonly used to treat human carcinomas with considerable antineoplastic activity specifically against ovarian, head, and neck carcinoma. PTX has also been effective treating lung cancer, breast cancer, acute leukemia and other solid tumors (Issels, 2008). Currently, the most common formulation of paclitaxel used in the clinical setting is Taxol™, which uses a carrier of Cremophor® EL and ethanol to increase the solubility of the highly hydrophobic drug. PTX and hyperthermia have a complex relationship in the treatment of cancer in that their combined effect is both cell-line dependent and there is variable effectiveness in the hyperthermia temperatures utilized (Issels, 2008). The objective of this work was to fabricate and characterize biodegradable PBAE-based hydrogel nanocomposites for the combined delivery of heat and paclitaxel. The degradation of the hydrogels allows for the controlled release of paclitaxel, whereas the iron oxide nanoparticles in the hydrogel matrix allow for the remote heating of the systems via an AMF. These systems could be implemented as a bulk material injected at a tumor site or implanted within a tumor resection site for the local delivery of anti-cancer therapeutics.

2. Materials and methods

2.1. Materials

Diethylene glycol diacrylate was obtained from Polysciences (Warrington, PA). Fe_3O_4 nanoparticles (20–30 nm diameter, 0.2% polyvinylpyrrolidone-coated) were obtained from Nanostructured and Amorphous Materials (Los Alamos, NM). Paclitaxel (99.5%) was from LC Laboratories (Woburn, MA). Ammonium persulfate (APS), isobutylamine (IBA), Cremophor® EL, Tween® 20, tetrahydrofuran, and poly(ethylene glycol) (N = 400) diacrylate (PEG400DA) were obtained from Sigma–Aldrich (St. Louis, MO). Cells and cell medium were obtained from American Type Culture Collection (Manassas, VA). The mammalian cell live/dead assay was from Molecular Probes/Invitrogen (Carlsbad, CA). All materials were used as received.

2.2. Synthesis and characterization of poly(β-amino ester) macromers

Two biodegradable poly(β-amino ester) macromers were synthesized via Michael addition reactions of IBA with excess poly(ethylene glycol) (PEG) diacrylate in a solvent-free manner. For one macromer, a 1:1.2 molar ratio of IBA to diethylene glycol diacrylate (DEGDA) (with 2 ethylene glycol units, n = 2) was reacted for 48 h at 85 °C with mixing (thereby denoted as 2EG–IBA). The second macromer was composed of a 1:1.2 molar ratio of IBA to PEG400DA (9 EG units, n = 9) reacted for 15 h at 85 °C (denoted 9EG–IBA). These compounds and the resulting macromer structure can be seen in Fig. 1. The macromers were then analyzed via a Shimadzu gel permeation chromatography (GPC) system to determine the average molecular weight and polydispersity index (PDI). The analysis was completed at 0, 24, and 48 h for the 9EG–IBA macromer and 0 and 15 h for the 2EG–IBA macromer. Attenuated Total Reflectance Fourier Transform Infrared (ATR-FTIR) analysis was performed to determine the conversion of available carbon–carbon double bonds present in the PEG diacrylate constituents of the macromers using a Varian Inc. 7000e step-scan spectrometer. A sample of the macromer solution was placed on the diamond ATR crystal and IR spectra were obtained at 8 cm^{-1} spectral resolution between 700 and 4000 cm^{-1}.

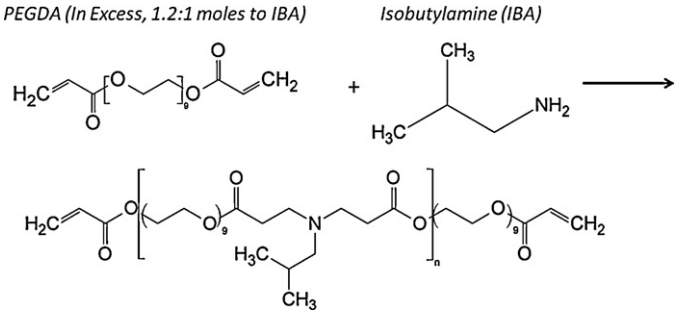

Fig. 1. Schematic for synthesis reaction of PBAE macromers composed of excess poly(ethylene glycol) (n) diacrylate with isobutylamine resulting in diacrylate-terminated structure. This structure has C=C bond end groups, allowing them to be reacted into hydrogel nanocomposites via free-radical initiation. These macromers are biodegradable due to hydrolysis of the available ester bonds present.

2.3. Fabrication of poly(β-amino ester)/iron oxide hydrogel nanocomposites

Magnetic hydrogel nanocomposites were fabricated via chemically-initiated, free-radical polymerization with various ratios of the two crosslinkable macromers, resulting in hydrogels with differing degradation profiles. The resulting systems had 0, 25, 50, 75, and 100 wt.% 2EG–IBA to 9EG–IBA macromer (100:0, 75:25, 50:50, 25:75, and 0:100 2EG–IBA). 5 wt.% iron oxide nanoparticles and 5 mg of paclitaxel per mg of macromer were added to the macromer solution which was exposed to ultrasonication (using a Fisher Brand Model 500 at a setting of 20% power) for 15 min using a probe placed in the middle of the macromer solution to facilitate dispersion of the nanoparticles and drug. After sonication, 1.5 wt.% of APS dispersed in water (2 mL water per gram of APS) was added to the mixture to initiate the free-radical polymerization in bulk with minimal water present. The solution was then vortexed before being loaded into a template consisting of two glass plates with a 1.5 mm thick Teflon spacer. Gels without paclitaxel used for cytotoxicity analysis were made the same way as described with paclitaxel, but without the chemical added. The systems were allowed to gel at least 12 h to allow for completion of polymerization.

2.4. Characterization of hydrogel nanocomposite degradation and swelling response

After polymerization, the hydrogels were cut into 8.2 mm diameter discs. The initial mass of each gel (m_i) was recorded and the gels were placed in individual tissue cassettes in a small container with PBS (pH 7.4). The cassettes were then placed in an incubator shaker at 37 °C and 100 rpm. The gels were removed at given times, their mass was recorded in their swollen state (m_s), and they were lyophilized to remove any residual water. Their mass was then measured in their dry state (m_d). The mass loss of the hydrogels was characterized by calculating the mass fraction remaining:

$$\text{mass fraction remaining} = \frac{m_d}{m_i} \quad (1)$$

The swelling of the gels was then characterized by the mass swelling ratio (q):

$$q = \frac{m_s}{m_d} \quad (2)$$

2.5. Mechanical testing: determination of compressive modulus

Compressive modulus of the hydrogel nanocomposites was determined with compressive mechanical testing. Gels were cut and placed in individual tissue cassettes in a small container with PBS (pH 7.4) and were then placed in an incubator shaker at 37 °C and 100 rpm for 30 s to allow for swelling and washing of unreacted PEGDA, IBA, and APS. The gels were tested using the displacement method on a BOSE ElectroForce 3300 with 1 mm displacement at a displacement rate of 0.05 mm/s with a 500 N load. Stress versus strain data were plotted and a linear strain range of 0.05–0.10 was analyzed for each gel. From this information, the compressive modulus of the gel was determined from the slope of the stress versus strain plot.

2.6. Iron oxide loss studies via thermogravimetric analysis

Thermal gravimetric analysis was completed to determine the actual iron oxide nanoparticle loading in the hydrogel nanocomposites as they degraded as this has the potential to affect the heating capability of the hydrogels. The 0:100 2EG–IBA (pure 9EG–IBA) hydrogel system was analyzed as a representative sample as it has the fastest degradation profile. A Netzsch STA 449A system (NETZSCH Instruments Inc., Burlington, MA) was used to perform this analysis. From an initial temperature of 20 °C, the gel samples were heated up to 120 °C at 5 °C/min, kept at 120 °C for 20 min to allow for water evaporation, and then heated up to 590 °C at 3 °C/min. The remaining mass was recorded.

2.7. Remote-controlled heating of PBAE hydrogel nanocomposites via an AMF

The magnetic hydrogel nanocomposites were heated using an AMF at different times throughout degradation to show their potential to heat and the effect of degradation on their heating properties. Prior to heating, hydrogel nanocomposites were cut into discs 8.2 mm in diameter. The hydrogels were initially heated in their dry state prior to beginning degradation. Gels were placed in individual tissue cassettes in a small container with PBS (pH 7.4) and were then placed in an incubator shaker at 37 °C and 100 rpm. Remote-controlled heating of the hydrogel nanocomposites was completed via an AMF induced by a Taylor Winfield induction power supply (model MMF-3-135/400-2) equipped with a solenoid with a 15 mm diameter and 5 turns. A schematic of the heating set-up can be seen in Fig. 5a. After a specified time, the hydrogel discs in their wet state were covered with Saran wrap, placed on top of the solenoid coil and exposed to the alternating magnetic field at 294 kHz and 17.4 kA/m. Thermal images and data were acquired using an infrared camera (AGEMA Thermovision 470) which recorded the surface temperature of the hydrogels. The surface temperature was recorded continuously for 5 min. The resulting data included the change in temperature (ΔT) from the initial temperature, as this would be the heating potential of the hydrogel despite the initial starting temperature.

2.8. Characterization of paclitaxel release

The release of paclitaxel from the hydrogel nanocomposites was measured via reverse-phase high performance liquid chromatography (HPLC). 8.2 mm samples were cut and placed in 3 mL of a modified PBS-based release medium composed of PBS, 2.4 wt.% Tween® 20, and 4 wt.% Cremophor® EL. The release took place at 37 °C and 100 rpm in an incubator shaker, and the gels were periodically placed in fresh medium to maintain infinite sink conditions. Prior to HPLC analysis, 2 mL of acetonitrile were added to each tube to ensure complete solubility of PTX in the solution. HPLC was performed using a Thermo Finnigan Spectra System with ChromQuest 4.0 software for data analysis. The mobile phase consisted of acetonitrile and water (50:50) with a 20 μL injection volume and 1.0 mL/min mobile phase flow rate. The separation was achieved using a reverse-phase C-18 Symmetry column (4.6 mm × 150 mm, 5 μm pore size) from Waters Corporation. The column eluate was evaluated at 227 nm for the detection of paclitaxel.

2.9. Cytotoxicity analysis of PBAE hydrogel nanocomposite degradation products

The degradation products of the hydrogel nanocomposites were analyzed for their cytotoxic effects. NIH 3T3 murine fibroblasts obtained from American Type Culture Collection (ATCC) were used. The complete culture medium included Dulbecco's Modified Eagle's Medium supplemented with 10% (v/v) calf bovine serum, 100 I.U./mL penicillin, 100 μg/mL streptomycin, and 1 μg/mL antimycotic Fungizone®. The fibroblasts were cultured at 37 °C and 5% CO_2 in a humidified incubator and were used from passages 4 through 8. Hydrogel nanocomposites with no paclitaxel were allowed to completely degrade in PBS. The degradation

Table 1
Molecular weight (MW) and polydispersity index (PDI) of macromers from gel permeation chromatography analysis. 15 and 48 h denote the final reaction time for the 2EG–IBA and 9EG–IBA systems, respectively.

System	Time (h)	MW	PDI
2EG–IBA	15	2206	1.9
9EG–IBA	24	2103	2.6
9EG–IBA	48	3663	3.0

products were then diluted to concentrations of 0.15, 1.5 and 4.5 mg/mL of degradation products to total medium amount. The resulting solutions were composed of 25% (v/v) PBS to complete cell medium. 25% (v/v) PBS to medium acted as the control. The fibroblasts were seeded at 17,500 cells/mL in 35 mm Petri dishes and were placed in an incubator for 24 h. The medium was removed from the Petri dishes and replaced with the hydrogel degradation product media samples for 48 h.

The viability of the fibroblasts was determined by counting the live and dead cells after 48 h using a Cellometer® Automated Cell Counter from Nexcelom Biosciences (Lawrence, MA). Initially, medium from each Petri dish was removed and collected in individual centrifuge tubes. The fibroblasts were then trypsinized and transferred to the corresponding centrifuge tubes and centrifuged to collect the cell pellet. After the supernatant was removed, 0.5 mL of Molecular Probes Live/Dead assay solution was added to the tube, the cells were resuspended in the solution, and placed in an incubator at 37 °C for at least 20 min before counting with the Cellometer®. The Live/Dead assay solution was composed of calcein AM which fluorescently stains live cells green and ethidium homodimer-1, which stains dead cells red. The cell viability was then calculated as the number of live cells over the total number of live and dead cells.

2.10. Statistical analysis

All experiments were performed at least in triplicate. MYSTAT 12 for Windows (12.02.00) was used for *t*-tests (paired *t*-test with unequal variances) to determine any significance in observed data. A *p*-value of <0.05 was considered statistically significant.

3. Results and discussion

3.1. Synthesis and characterization of poly(β-amino ester) macromers

PBAE macromers composed of excess PEGDA with isobutylamine were synthesized via a Michael addition reaction resulting in macromer chains with diacrylate endchain groups (as seen in Fig. 1) allowing for their crosslinking into hydrogel matrices. GPC was used to analyze the molecular weight and PDI of the macromers as seen in Table 1.

For the 2EG–IBA macromer, the average molecular weight after 15 h (completion of reaction) was 2206 g/mol whereas for the 9EG–IBA macromer, the molecular weight increased with reaction time ranging from 2103 g/mol at 24 h to 3663 g/mol after 48 h (completion of reaction). The PDI values were 1.9 for the 2EG–IBA macromer and 2.6 and 3.0 for the 9EG–IBA macromer after 24 and 48 h reaction times. These values increased with reaction time resulting in a broader range of macromer chain lengths within the macromers. The increase of PDI with time can be rationalized as being a result of unreacted PEGDA components, the reaction of smaller macromer chains to form larger chains, or a combination of both. ATR-FTIR was used to determine the conversion of carbon–carbon double bonds present in the PBAE macromers. As the macromer reaction occurs, the C=C bonds react with IBA, decreasing the C=C peak at 1637 cm^{-1} which is confirmed in the IR spectra. This peak does not completely disappear, however, as the final macromer product has available C=C bonds from the PEGDA due to it being present in excess during the macromer synthesis. The conversion of the hydrogel nanocomposites was not analyzed via FTIR due to difficulty in resolving the carbon double bond peak. All gels were solid with minimal fluid indicating near complete conversion of the hydrogel systems. Both the GPC and IR spectra are provided in Appendix A, Figs. A.1 and A.2, respectively.

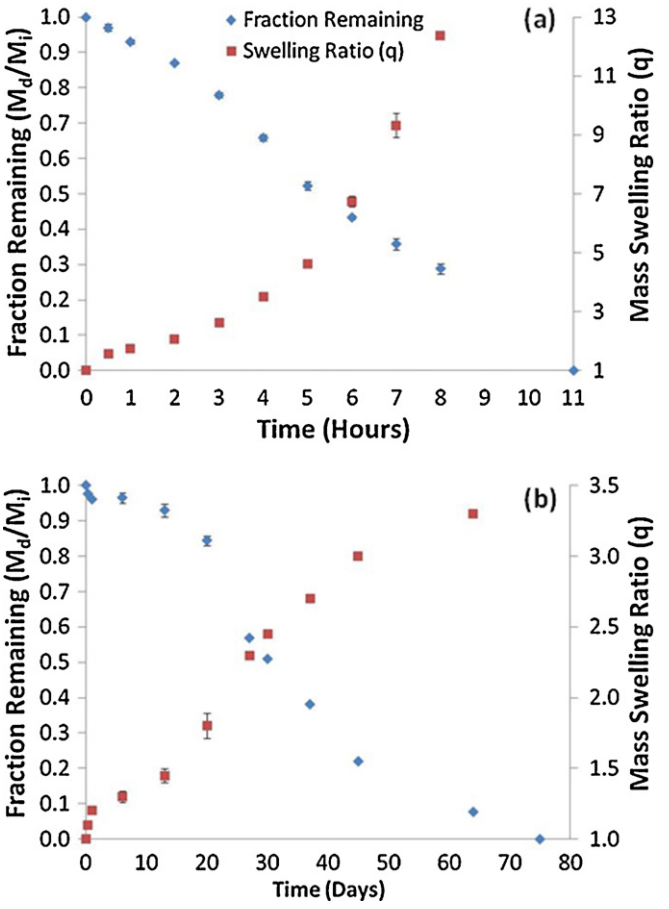

Fig. 2. Mass fraction remaining and mass swelling ratio (q) data for: (a) 0:100 and (b) 100:0 2EG–IBA magnetic hydrogel nanocomposites with time. Blue diamonds correspond to the fraction remaining (m_d/m_i) on the left x-axes and red squares correspond to the volume swelling ratios (q) on the right x-axes. $N = 3 \pm$ SE. (For interpretation of the references to color in this figure legend, the reader is referred to the web version of the article.)

3.2. Hydrogel nanocomposite degradation and swelling response

Magnetic hydrogel nanocomposites were fabricated via free-radical polymerization resulting in a biodegradable hydrogel system. Degradation studies were completed for hydrogels based on 0, 25, 50, 75, and 100 wt.% 2EG–IBA to 9EG–IBA macromers. Fig. 2 shows both the fractional mass remaining and mass swelling ratio of the hydrogel nanocomposites with respect to time.

The 0:100 2EG–IBA hydrogels completely degraded in approximately 11 h whereas the 100:0 2EG–IBA hydrogels completed degraded in approximately 75 days. Additionally, 25:75, 50:50, and 75:25 2EG–IBA hydrogels completely degraded in approximately 5, 15, and 68 days. The final data were not collected due to the difficulty in handling the hydrogels near the end time points and the end of the degradation time for all systems was determined via visual observations. The faster degradation of the 0:100 2EG–IBA

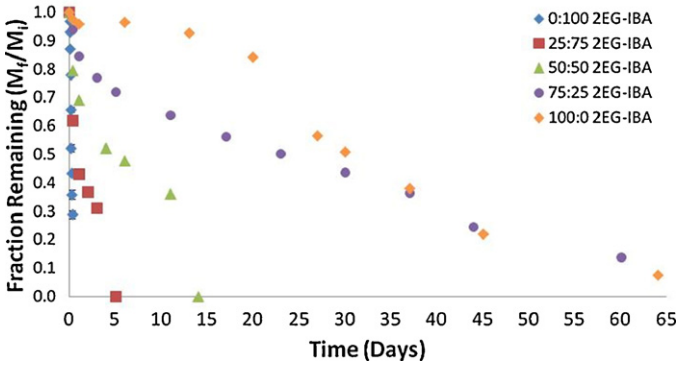

Fig. 3. Mass fraction remaining data for all magnetic hydrogel nanocomposites over time including the degradation data for the systems in Fig. 2 as a comparison for all systems. $N = 3 \pm$ SE.

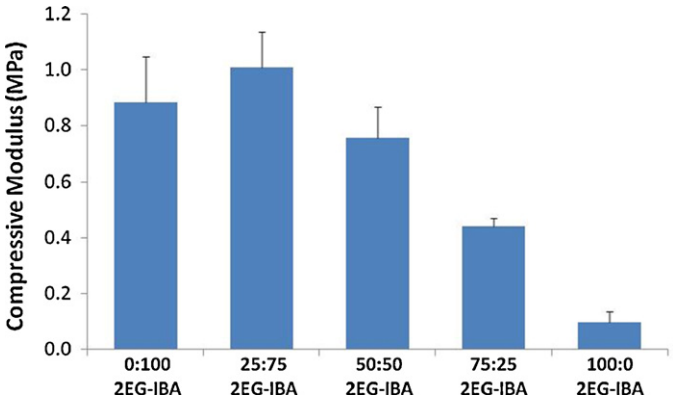

Fig. 4. Compressive modulus data for magnetic hydrogel nanocomposites after exposure to PBS at 37 °C. $N = 3 \pm$ SD.

hydrogel is a result of the presence of more ethylene glycol groups in the macromer backbone in comparison to the 100:0 2EG–IBA hydrogel, resulting in a more hydrophilic macromer and resulting hydrogel. The mass fraction curve was slightly sigmoidal-shaped for all hydrogels. This profile is likely due to the broad PDI of both macromers resulting in both shorter and longer chains present in the macromer which results in differing degradation profiles, affecting the initial and final degradation response of the systems.

The mass swelling ratio (q) of the hydrogels increased with time as seen in Fig. 2. This is due to the continued degradation of the gels with time which results in breakage of the crosslinking in the hydrogel matrix allowing for increased water content. 0:100 2EG–IBA hydrogel (containing only 9EG–IBA macromer) had the highest mass swelling ratio with time (12.4), and the final mass swelling ratios for the other hydrogels decreased with increasing 2EG–IBA content (3.3 for 100:0 2EG–IBA). This is due to the increase in hydrophobicity due to 2EG–IBA. The hydrogels exhibited bulk degradation as evidenced by their increased swelling with continued degradation.

Fig. 3 shows a comparison of the fractional mass remaining of all of the hydrogel systems. Decreasing the amount of 2EG–IBA macromer resulted in faster degrading systems due to the decrease in hydrophobicity of the hydrogel systems. The 75:25 and 100:0 2EG–IBA hydrogel exhibited similar final degradation time which is likely a result of the 9EG–IBA macromer initially degrading quickly out of the 75:25 2EG–IBA hydrogel causing it to behave similarly to the 100:0 2EG–IBA gel after approximately 35 days. Also, the 100:0 2EG–IBA system exhibited a significant lag in degradation initially in comparison to the other systems. This could be due to the hydrophobicity of the macromer preventing water penetration in the hydrogel initially, which decreased the degradation rate. Overall, this data shows the ability to tailor the degradation and swelling profiles of these hydrogels by adjusting the macromer content.

3.3. Mechanical testing: determination of compressive modulus

Compression testing was performed on all PBAE hydrogel systems at an initial time point after 30 min in PBS at 37 °C. This data can be seen in Fig. 4 where the hydrogels with higher 9EG–IBA content exhibited a greater compressive modulus. This is likely due to the fact that residual PEG400DA is present in the 9EG–IBA macromer which produces highly crosslinked regions throughout the gel. This phenomenon has been demonstrated by Hawkins et al. (Hawkins et al., 2011a,b) where heterogeneous macromers produced densely crosslinked regions composed primarily of PEG. Also, the 0:100 2EG–IBA system exhibited a lower modulus initially which is likely a result of it already degrading slightly more than the other gels after 30 min.

3.4. Iron oxide loss studies via thermogravimetric analysis

TGA was performed to determine the actual amount of iron oxide nanoparticles present in the hydrogel nanocomposites as they degraded. Samples were analyzed at 0, 0.5, 3, and 8 h for the 0:100 2EG–IBA hydrogel systems as a representation of what occurs in the remaining hydrogel nanocomposites. The resulting % iron oxide values based on the dry hydrogel nanocomposite mass were 4.9, 4.7, 5.3, and 12.4% with respect to the times recorded above. As time and amount of degradation increased, the mass % of the iron oxide in the nanocomposites (iron oxide to polymer amount) increased. The polymer degradation byproducts were able to diffuse more readily out of the hydrogels than the iron oxide nanoparticles themselves. The effect of this phenomenon will be discussed further in the next section concerning the remote-controlled heating of the hydrogel nanocomposites.

3.5. Remote-controlled heating of PBAE hydrogel nanocomposites via an AMF

PBAE hydrogel nanocomposites can potentially be used in hyperthermia applications where heating of the magnetic hydrogel matrix can be achieved by exposure to an alternating magnetic field. This phenomenon is due to the Fe_3O_4 nanoparticles present in the hydrogel matrix. In these studies, the swollen hydrogels were exposed to an electromagnetic field for 5 min at 294 kHz and 17.4 kA/m to induce heating within the systems for the following conditions: dry hydrogels and hydrogels after degradation at various time points. As seen in Fig. 5 for the 0:100 2EG–IBA hydrogel system, the hydrogels were able to heat for all conditions, and the maximum change in temperature reached decreased as the gels degraded. For all conditions, the temperature differentials reached (31–55 °C) are well beyond the required values for hyperthermia (a ΔT value of 5–6 °C), indicating that the nanocomposites could be used for hyperthermia applications. As demonstrated in other studies (Meenach et al., 2009c), the heating of hydrogel nanocomposites can be controlled by the power of the alternating magnetic field to induce the temperature range necessary for hyperthermia despite the condition of the hydrogel system.

This response was similar for the other four hydrogel systems (data not reported). The amount of heating of the hydrogel systems is dependent on multiple factors including the amount of iron oxide present in the gel volume and the amount of water present in the gels, which can dissipate the heat generated by the iron oxide nanoparticles. Table 2 shows the relationships between the ΔT values (final versus initial temperature during heating), mass swelling ratio (q), fractional mass remaining (from degradation data), TGA-based iron oxide mass % (amount of iron oxide per total gel mass),

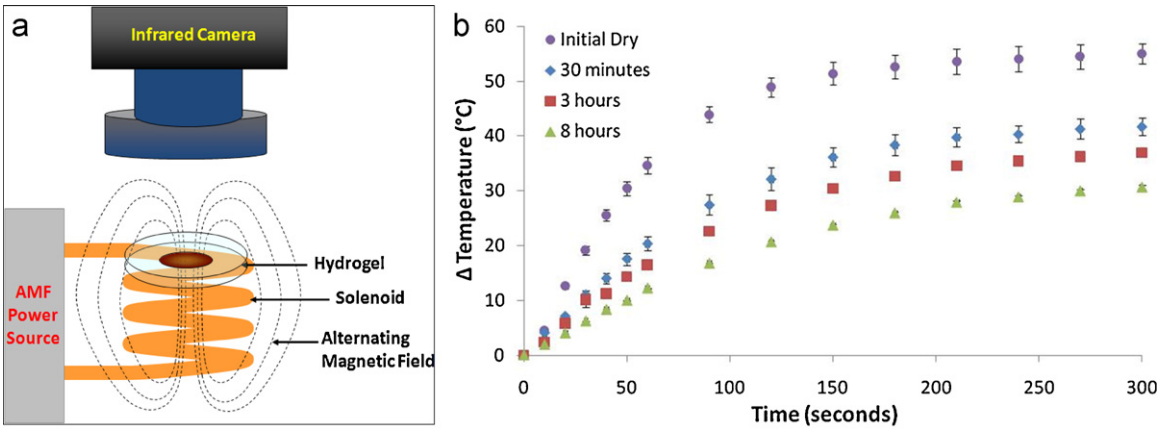

Fig. 5. (a) Schematic of alternating magnetic field setup and (b) thermal analysis of 0:100 2EG–IBA magnetic hydrogel nanocomposite with time upon exposure to an alternating magnetic field at 17.4 kA/m and 294 kHz for 5 min ($N = 3 \pm SD$).

Table 2
Comparison of mass swelling ratio (q value), fraction of mass remaining, final temperature of hydrogel surface temperature after 5 min exposure to an AMF, iron oxide loading amount from TGA data, and the calculated mass of iron oxide remaining for the 0:100 2EG–IBA hydrogel system with time/degradation.

Time	Final ΔT (°C)	q value	Fraction mass remaining	% Iron oxide	Actual Fe_3O_4 mass remaining (mg)	Theoretical Fe_3O_4 mass remaining (mg)
Initial	55.0 ± 1.9	1.00	1.00	4.9 ± 0.1	4.4 ± 0.0	4.5
30 min	41.8 ± 1.6	1.6 ± 0.0	0.97 ± 0.01	4.7 ± 0.0	4.1 ± 0.0	4.4
3 h	36.9 ± 0.5	2.6 ± 0.1	0.78 ± 0.01	5.3 ± 0.1	3.7 ± 0.1	3.5
8 h	30.6 ± 0.4	12.4 ± 0.1	0.29 ± 0.01	12.4 ± 0.2	3.2 ± ± 0.1	1.3

and average iron oxide mass remaining values from each gel. The mass remaining values were calculated as follows:

$$Fe_3O_4 \text{ mass remaining} = m_d \times \text{fraction mass remaining} \times \% \text{ iron oxide} \quad (3)$$

where m_d is the mass of the dry hydrogel from the degradation analysis. The % iron oxide value used in the calculation is the experimental value from the TGA data for the actual iron oxide mass remaining and the theoretical value (5% based on the loading amount) for the theoretical iron oxide mass remaining.

With time, the mass swelling ratio increased with degradation allowing for more water to enter the hydrogels. Upon examining the resulting TGA data, the % iron oxide remaining in the hydrogel increased as the hydrogel degradation. While this seemed counter-intuitive, upon examination of the data, the actual iron oxide mass calculated indicated that the iron oxide mass decreased, which is what was expected based on the theoretical data. Despite this, the actual iron oxide amount remaining in a hydrogel sample was greater than the theoretical. This could possibly be explained in that though the hydrogel polymer matrix is degrading in a bulk fashion, the decrease in polymer chains may not be enough for the iron oxide particles to also leach out of the system. Therefore, the polymer degrades out faster, leaving more nanoparticles behind. This could be beneficial for a hyperthermia application in that with more iron oxide present, a lower magnetic field strength would be necessary to induce the required temperature. Overall, both the increased in water content of the hydrogels and decrease in iron oxide mass throughout the system resulted in a decrease in the heating of the hydrogels with time.

3.6. Characterization of paclitaxel release

In order to evaluate the ability of PBAE hydrogels to effectively deliver paclitaxel, in vitro release studies were performed in a PBS solution containing 2.4 wt.% Tween® 20 and 4 wt.% Cremophor® EL at 37 °C and 100 rpm. The PTX concentrations were determined using a standard curve from the PTX concentration and HPLC data in a 60:40 (v/v) release medium to acetonitrile solution (data not shown). Fig. 6 shows the release profile of PTX from the PBAE hydrogels.

The PTX was continuously released from the hydrogels, and a near-zero-order release was initially evident for all hydrogel systems. After approximately 60–70% release, the PTX release slowed for most systems. Similar to the degradation data, the 100 9EG–IBA released paclitaxel the fastest due to its higher hydrophilicity in comparison with the gels containing 2EG–IBA macromer. This data suggests that these hydrogels have the potential to be used as good controlled drug delivery carriers, and the drug release time can be controlled by the degradation rate of the hydrogel system. One advantage of using such materials to release paclitaxel is that they could be delivered directly to the tumor site via an injection of the hydrogel system prior to gel formation, overcoming solubility issues present in the systemic delivery of the drug. Degradation of the hydrogels would control the release of the paclitaxel and prevent premature release of the drug.

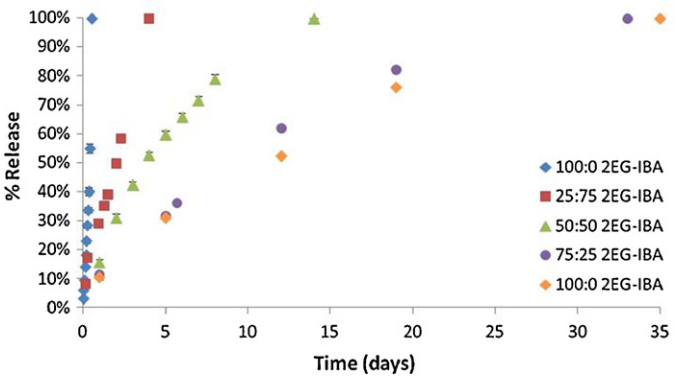

Fig. 6. Analysis of paclitaxel release from hydrogel nanocomposites over time via HPLC. $N = 3 \pm SE$.

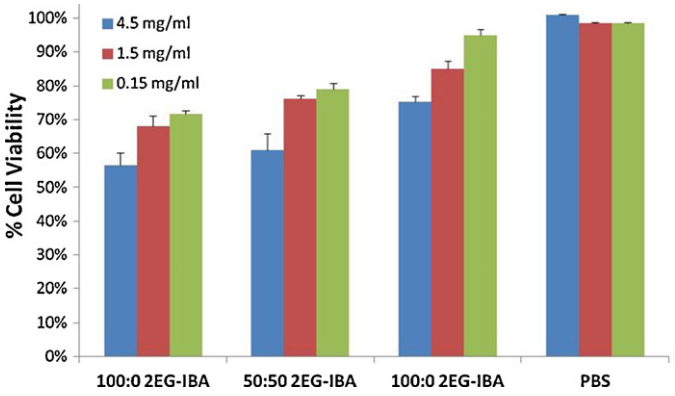

Fig. 7. Cytotoxicity analysis of NIH 3T3 murine fibroblasts exposed to completely degraded PBAE hydrogel nanocomposites at various concentrations for 48 h. $N = 3 \pm SE$.

3.7. Cytotoxicity analysis of PBAE hydrogel nanocomposite degradation products

Cytotoxicity analysis of the PBAE hydrogel nanocomposite degradation products was analyzed as the hydrogels can potentially be used as implantable or injectable in vivo drug delivery depots. Hydrogels without paclitaxel but with iron oxide nanoparticles were completely degraded in PBS. These solutions were then diluted to 0.15, 1.5, and 4.5 mg/mL in 25% (v/v) PBS to cell medium. NIH 3T3 fibroblasts were then exposed to these solutions for 48 h, and their cytotoxicity was analyzed using a Cellometer® Automater Cell Counter. Fig. 7 shows the % cell viability (number of live cells versus total number cells) for 100:0 2EG–IBA, 50:50 2EG–IBA, 0:100 2EG–IBA, and a PBS control.

For all hydrogels, the cell viability decreased with increasing degradation product concentration. Additionally, the viability was greater with increasing 9EG–IBA content. Overall, these results show differences in cell viability for different conditions, and in vivo evaluation will be necessary to show the overall safety of these systems. However, this does show the potential for safety with the correct degradation product clearance from the implantation site. Once the clearance rate and amount of the degradation products was determined, the safety could be better evaluated.

4. Conclusion

Magnetic PBAE-based hydrogel nanocomposites have the ability to successfully deliver both heat and the chemotherapeutic agent, paclitaxel, in a controlled manner. Both the degradation and PTX release profiles can be tailored based on the type of macromer used with the more hydrophilic hydrogel system (0:100 2EG–IBA) degrading in 11 h versus over nearly 7 weeks for the more hydrophobic system (100:0 2EG–IBA). The paclitaxel release was controlled by the degradation of the hydrogels through bulk degradation. The heating capability of the hydrogels when exposed to an AMF decreased as the hydrogels degraded. This is due to an increase in their swelling (and therefore increase in water content) and decrease in the amount of iron oxide present in the hydrogels with time. The degradation products exhibited cell viabilities ranging from 53 to 92% depending on the type of hydrogel and concentration of degradation products. Overall, these systems have the potential to be used as implanted or injected drug (and heat) delivery depots for the synergistic treatment of cancer.

Acknowledgments

Partial funding for this research was provided by the Kentucky Science and Engineering Foundation (Award Number KSEF0148-502-06-188). S. Meenach and J. Shapiro acknowledge the Engineered Bioactive Interfaces & Devices NSF IGERT (Award Number DGE-0653710) and NSF IGERT REU (Award Number EEC-0851716) for providing partial funding for this research, respectively.

Appendix A.

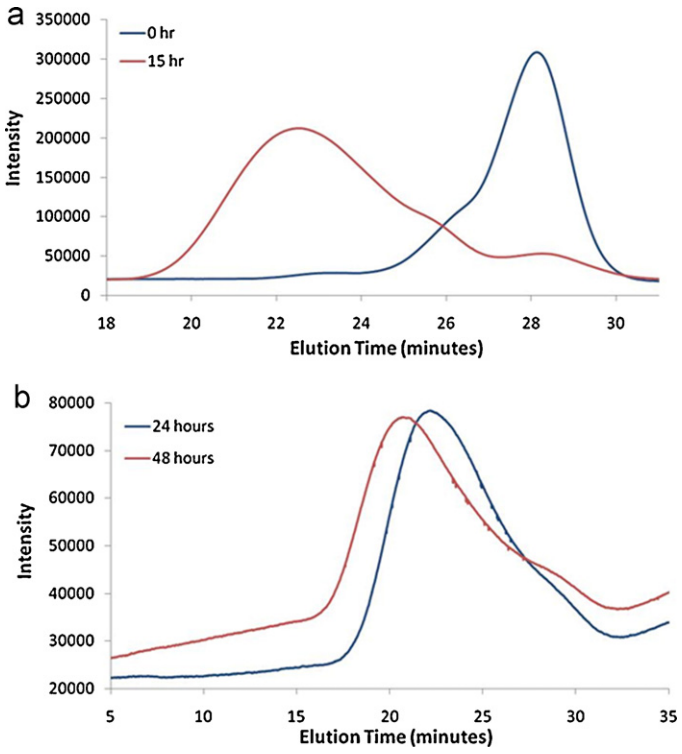

Fig. A.1. Gel permeation chromatograms for PBAE macromers where (a) is for 1:1.2 diethylene glycol diacrylate to isobutylamine (2EG–IBA) for 0 and 15 h and (b) is for 1:1.2 poly(ethylene glycol) ($n = 9$) diacrylate to isobutylamine (9EG–IBA) at 24 and 48 h.

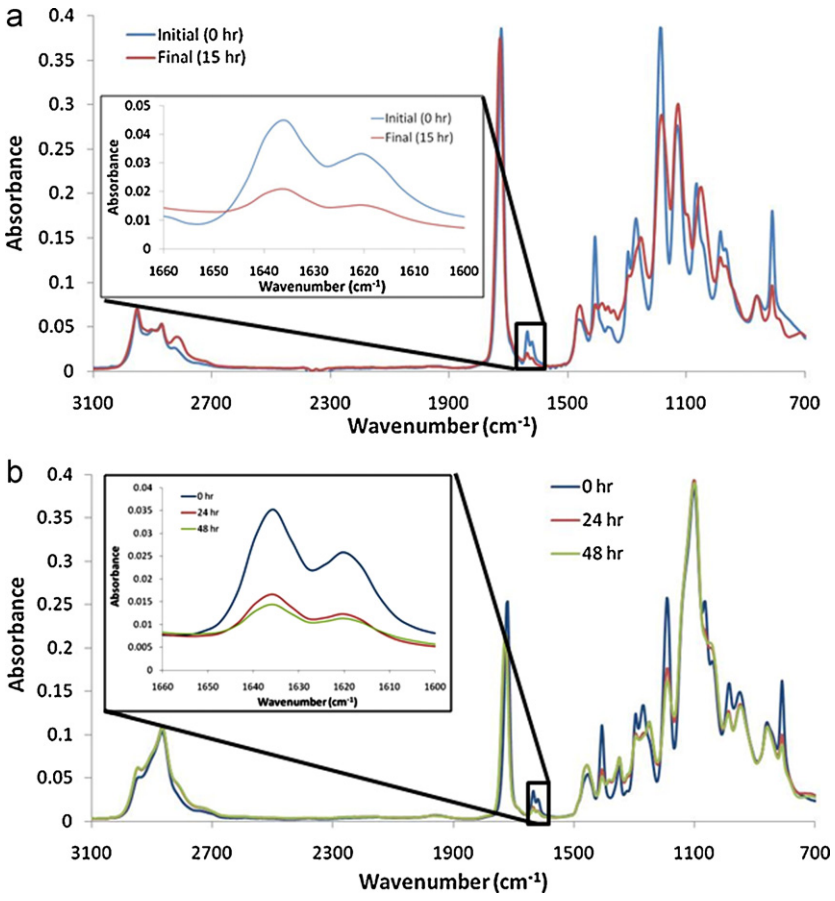

Fig. A.2. ATR-FTIR spectra of 2EG–IBA macromer (1:1.2 diethylene glycol diacrylate:isobutylamine) spectra before and after synthesis (0 and 15 h).

References

ACS, 2009. Cancer Facts and Figures. American Cancer Society.

Anderson, D.G., Tweedie, C.A., Hossain, N., Navarro, S.M., Brey, D.M., Van Vliet, K.J., Langer, R., Burdick, J.A., 2006. A combinatorial library of photocrosslinkable and degradable materials. Adv. Mater. 18, 2614–2618.

Babincova, M., Leszczynska, D., Sourivong, P., Cicmanec, P., Babinec, P., 2001. Superparamagnetic gel as a novel material for electromagnetically induced hyperthermia. J. Magn. Magn. Mater. 225, 109–112.

Falk, M.H., Issels, R.D., 2001. Hyperthermia in oncology. Int. J. Hyperthermia 17, 1–18.

Guedes, M.H.A., Sadeghiana, N., Lima, D., Peixoto, G., Coelho, J.P., Barbosa, L.S., Azevedo, R.B., Kuckelhaus, S., de Fatima Da Silva, M., Morais, P.C., Lacava, Z.G.M., 2005. Effects of AC magnetic field and carboxymethyldextran-coated magnetite nanoparticles on mice peritoneal cells. J. Magn. Magn. Mater. 293, 283–286.

Hawkins, A.M., Milbrandt, T.A., Puleo, D.A., Hilt, J.Z., 2011a. Synthesis and analysis of degradation, mechanical and toxicity properties of poly(beta-amino ester) degradable hydrogels. Acta Biomater. 7, 1956–1964.

Hawkins, A.M., Puleo, D.A., Hilt, J.Z., 2011b. Effect of macromer synthesis time on the properties of the resulting poly(beta-amino ester) degradable hydrogel. J. Appl. Polym. Sci. 122, 1420–1426.

Hawkins, A.M., Satarkar, N.S., Hilt, J.Z., 2009. Nanocomposite degradable hydrogels: demonstration of remote controlled degradation and drug release. Pharm. Res. 26, 667–673.

Hildebrandt, B., Wust, P., Ahlers, O., Dieing, A., Sreenivasa, G., Kerner, T., Felix, R., Riess, H., 2002. The cellular and molecular basis of hyperthermia. Crit. Rev. Oncol. Hematol. 43, 33–56.

Issels, R.D., 2008. Hyperthermia adds to chemotherapy. Eur. J. Cancer 44, 2546–2554.

Meenach, S.A., Anderson, A.A., Suthar, M., Anderson, K.W., Hilt, J.Z., 2009a. Biocompatibility analysis of magnetic hydrogel nanocomposites based on poly(N-isopropylacrylamide) and iron oxide. J. Biomed. Mater. Res. A 91A, 903–909.

Meenach, S.A., Anderson, K.W., Hilt, J.Z., 2009b. Hydrogel nanocomposites: biomedical applications, biocompatibility and toxicity analysis. In: Webster, T.J. (Ed.), Safety of Nanoparticles. Springer, New York, pp. 131–157.

Meenach, S.A., Hilt, J.Z., Anderson, K.W., 2009c. Poly(ethylene glycol)-based magnetic hydrogel nanocomposites for hyperthermia cancer therapy. Acta Biomater. 6, 1039–1046.

Michalakis, J., Georgatos, S.D., de Bree, E., Polioudaki, H., Romanos, J., Georgoulias, V., Tsiftsis, D.D., Theodoropolous, P.A., 2007. Short-term exposure of cancer cells to micromolecular doses of Paclitaxel, with or without hyperthermia, induces long-term inhibition of cell proliferation and cell death in vitro. Ann. Surg. Oncol. 14, 1220–1228.

Moroz, P., Jones, S.K., Gray, B.N., 2002. Magnetically mediated hyperthermia: current status and future directions. Int. J. Hyperthermia 18, 267–284.

Obara, K., Ishihara, M., Ozeki, Y., Ishizuka, T., Hayashi, T., Nakamura, S., Saito, Y., Yura, H., Matsui, T., Hattori, H., Takase, B., Ishihara, M., Kikuchi, M., Maehara, T., 2005. Controlled release of paclitaxel from photocrosslinked chitosan hydrogels and its subsequent effect on subcutaneous tumor growth in mice. J. Control. Release 110, 79–89.

Peppas, N.A., Hilt, J.Z., Khademhosseini, A., Langer, R., 2006. Hydrogels in biology and medicine: from molecular principles to bionanotechnology. Adv. Mater. 18, 1345–1360.

Satarkar, N.S., Hilt, J.Z., 2008. Magnetic hydrogel nanocomposites for remote controlled pulsatile drug release. J. Control. Release 130, 246–251.

Satarkar, N.S., Zhang, W., Eitel, R.E., Hilt, J.Z., 2009. Magnetic hydrogel nanocomposites as remote controlled microfluidic valves. Lab-on-a-Chip 9, 1773–1779.

Sneed, P.K., Stauffer, P.R., McDermott, M.W., Diederich, C.J., Lamborn, K.R., Prados, M.D., Chang, S., Weaver, K.A., Spry, L., Malec, M.K., Lamb, S.A., Voss, B., Davis, R.L., Wara, W.M., Larson, D.A., Phillips, T.L., Gutin, P.H., 1998. Survival benefit of hyperthermia in prospective randomized trial of brachytherapy boost and hyperthermia for glioblastoma multiforme. Int. J. Radiat. Oncol. Biol. Phys. 40, 287–295.

Ta, H.T., Dass, C.R., Dunstanc, D.E., 2008. Injectable chitosan hydrogels for localised cancer therapy. J. Control. Release 126, 205–216.